의학박사 학위논문

# 막성신증에서 푸마르산이 phospholipase A2 수용체 자가면역에 의한 족세포 손상에 미치는 영향

Fumarate modulates phospholipase A2 receptor autoimmunity-induced podocyte injury in membranous nephropathy

2021 년 2 월

서울대학교 대학원

내과학 의학과

조 형 아
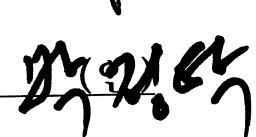
# 막성신증에서 푸마르산이 phospholipase A2 수용체 자가면역에 의한 족세포 손상에 미치는 영향

지도교수 김 동 기

이 논문을 의학박사 학위논문으로 제출함
2020 년  10 월

서울대학교 대학원
의학과 내과학
조 형 아

조형아의 박사 학위논문을 인준함
2021 년  1 월

위 원 장 _____ 주 권 욱 _____

부위원장 _____ 김 동 기 _____

위    원 _____ 김 현 경 _____

위    원 _____ 김 항 래 _____

위    원 _____ 박 정 탁 _____

Abstract

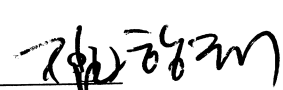# Fumarate modulates phospholipase A2 receptor autoimmunity-induced podocyte injury in membranous nephropathy

Hyung Ah Jo

Medicine, Internal medicine

The Graduate School

Seoul National University

Downstream mechanisms that lead to podocyte injury mediated by phospholipase A2 receptor (PLA2R) autoimmunity remain elusive. Accumulating evidence has been shown that increased production of reactive oxygen species (ROS) can cause podocyte injury. Also, the activation of the complement system which involved the ROS generation has been identified in membranous nephropathy (MN).

Among the molecules related to ROS, fumarate was recently known to be involved in the podocyte injury. Here, the role of fumarate in modulating phospholipase A2 receptor-mediated podocyte injury was investigated in *in vitro* model of PLA2R-associated MN.

Fumarate hydratase, which hydrolyzes fumarate, colocalized with podocalyxin, and its expression was lower in glomerular sections from patients with PLA2R-associated MN than in those from healthy individuals, patients with non-PLA2R associated MN or minimal change disease.

To elucidate the role of fumarate in podocyte injury in *in vitro* model of PLA2R-associated MN, the immunoglobulin G (IgG) was purified from the serum of patients with PLA2R-associated MN (MN-IgG) and a healthy control (Con-IgG). The purified MN-IgG reacted with the 153 kDa band when the lysates of primary cultured human podocytes were immunoblotted, but Con-IgG did not. Podocytes stimulated with MN-IgG decreased expression of fumarate hydratase and increased fumarate levels. These changes were coupled to alterations in the expression of molecules involved in the phenotypic profile of podocytes (WT1, ZO-1, Snail, and Fibronectin), an increase in albumin flux across the podocyte layer and the production of ROS in podocytes. However, overexpression of fumarate hydratase ameliorated these alterations. Furthermore, knockdown of fumarate hydratase exhibited synergistic effects with MN-IgG treatment. Thus, fumarate may promote changes in the phenotypic profiles of podocytes after the development of PLA2R autoimmunity.

These findings suggest that fumarate could serve as a potential target for the treatment of PLA2R-associated MN.

keywords : fumarate, PLA2R-associated membranous nephropathy, podocyte
*Student Number* : 2015-30559

# Contents

# List of Figures

hydratase activation lentiviral particles at 1 MOI, 2 MOI.
(C) Liquid chromatography-mass spectrometry analysis of the fumarate levels in the lysates of podocytes transduced with control lentiviral particles at 1 MOI for 6 hrs, control lentiviral particles at 1 MOI for 24  hrs, fumarate hydratase activation lentiviral particles at 1 MOI for 6 hrs, or fumarate hydratase activation lentiviral particles at 1 MOI for 24 hrs. ········ 42

# Introduction

## Clinical manifestations and the pathogenesis of anti-phospholipase A2 receptor-associated membranous nephropathy (PLA2R-associated MN)

Phospholipase A2 receptor (PLA2R)-associated membranous nephropathy (MN) is an autoimmune disease caused by autoantibodies against M-type PLA2R and is the most common cause of nephrotic syndrome in adults.[1] Given the exclusive and robust association of two loci, *PLA2R1* and *HLA-DQA1*, with the risk of the disease, PLA2R-associated MN may undoubtedly be genetically determined, unlike many other glomerular disease with polygenic risk factors.[2-4] Previous studies have also demonstrated that anti-PLA2R levels, which are profoundly influenced by high-risk genotypes, predict responsiveness to immunosuppressive treatment and renal outcomes in the majority of PLA2R-associated MN patients.[5-8] However, the mechanisms by which PLA2R-autoimmunity mediates podocyte injury remain unresolved. Furthermore, the significant proportion of the patients do not completely respond to non-specific immunosuppressive therapy having considerable side effects.[9,10] Therefore, the study to define the mechanism in which PLA2R-autoimmunity induced podocyte injury that might be therapeutic targets should be investigated. The present study investigate the pathogenesis of the

podocyte injury via *in vitro* experiments mimicking the PLA2R-associated MN milieu.

## Podocyte injury in PLA2R-associated MN

The main findings of Heymann nephritis, the experimental animal model of MN is the activation of the complement system accompanied by reactive oxygen species (ROS) on podocytes.[11] Also, the universal findings of C3 deposits in the kidney specimens from MN also suggests activation of complement system in the pathogenesis of the disease.[12] Accumulating evidence shows that complement activation within podocytes induces NADPH oxidase expression and further increases the production of ROS, which can cause functional impairment of podocytes.[13,14] These findings suggest that the potential mechanisms by which anti-PLA2R autoantibody induce podocyte injury may include the complement system activation accompanied by ROS and related molecules. Among the molecules related to ROS that induce podocyte injury, fumarate has previously known to involve the pathogenesis of diabetic nephropathy in experimental animal model.[15] Fumarate hydratase is a tricarboxylic cycle enzyme which converts malate to fumarate.[16] The inhibition of fumarate hydratase and increased production of fumarate has been known to involve the upregulation and stabilization of hypoxia-inducible factor protein.[17] These findings imply that decreased expression of fumarate hydratase and increased production of

fumarate might participate in the podocyte injury via ROS.

Therefore, this study aimed to investigate the role of fumarate leading the podocyte injury in *in vitro* model of PLA2R-associated MN. First, the glomerular expression of fumarate hydratase in the kidney biopsy specimens obtained from patients with PLA2R-associated MN was compared with those from disease controls including non-PLA2R/thrombospondin type 1 domain-containing 7A (THSD7A)-associated MN, minimal change disease (MCD), diabetic nephropathy and healthy controls. In the first part of the present study, *in vitro* model mimicking the milieu of PLA2R-associated MN was defined using purified immunoglobulin G obtained from the serum of the patients with PLA2R-associated MN and using the primary cultured human podocytes. The markers of filtration barrier integrity and podocyte differentiation were evaluated according to the administration of immunoglobulin G from a patient with a high titer of anti-PLAR autoantibody (MN-IgG) to the primary cultured human podocytes. The treatment of MN-IgG to the podocytes showed the lose of epithelial features accompanied by the acquirement of mesenchymal features of podocytes. These findings occurred with the attenuated expression of fumarate hydratase and increased levels of intracellular fumarate and ROS.

In the second part of this study, whether the overexpression of fumarate hydratase leading to the decreased level of fumarate in the podocytes could abrogate the effect of MN-IgG on podocyte injury was explored in *in vitro* model of PLA2R-associated MN.

Unfavorable changes in podocytes according to the MN-IgG treatment including phenotypic alteration, ROS production, and increased permeability to albumin across the podocyte layer were ameliorated by overexpression of fumarate hydratase. Next, whether the inhibition of fumarate hydratase leading to increased production of fumarate synergistically aggravated the MN-IgG induced podocyte injury was examined. In addition, the expression of fumarate hydratase following C5b-9 assembly treatment was investigated in *in vitro* podocytes to examine the effect of activation of complement system on the expression of fumarate hydratase. The pretreatment of the NADPH oxidase inhibitor was used to examine the effects of ROS on the expression of fumarate hydratase and zonula occludens-1 (ZO-1).

# Materials and Methods

## Study subjects and specimens

This study was conducted according to the Declaration of Helsinki and approved by the institutional board of Seoul National University Hospital, Seoul, Korea (IRB no. 1601-076-734). The human biospecimens of the study subjects were provided by the National Biobank of Korea.[18] The serum samples and kidney biopsy specimens were provided by the National Biobank of Korea (IRB no. 1004-037-315). The institutional Review Board of Seoul National University Hospital approved the protocols for obtaining serum samples and kidney biopsy specimens from patients with PLA2R-associated MN, non-PLA2R/THSD7A-associated MN, MCD, diabetic nephropathy and healthy controls, and kidney sections from patients who underwent nephrectomy because of renal cell carcinoma. Informed consent to collect serum samples and kidney biopsy specimens were obtained.

PLA2R-associated MN was defined as having positive serum anti-PLA2R antibodies or glomerular PLA2R antigen.[19] The serum anti-PLA2R level was assessed by ELISA (Euroimmun AG), and a positive result was defined as $\geq$ 20 RU/mL.[19] The results of PLA2R staining was defined as positive[19] if PLA2R staining was distributed along the glomerular capillary loops in a fine granular pattern and

colocalized with IgG4. Glomerular THSD7A deposits were measured using the immunohistochemistry method.[20]

# Detection of glomerular phospholipase A2 receptor antigen

To detect the glomerular PLA2R antigen, kidney biopsy tissues of patients with MN were deparaffinized, hydrated, and heated for 10 min at 120°C before being blocked with 10% fetal bovine serum (FBS) for 10 min. The antigens were conjugated using a rabbit polyclonal anti-human PLA2R antibody (Atlas Antibodies) followed by a FITC—conjugated swine anti-rabbit IgG antibody (Invitrogen). To detect glomerular IgG4 immune deposition, sheep anti-human IgG4 monoclonal antibody (Abcam) was used as the primary antibody followed by Alexa 488— and 555—conjugated probes (Invitrogen). Stained samples were evaluated by confocal microscopy (Leica TCS SP8, Leica Microsystem GmbH) and analyzed using Leica Imaris 7.6 (Leica Microsystem GmbH).

# *In vitro* experiments
# Primary cultured human podocytes

Human primary cultured human podocytes were harvested as previously reported.[21] Kidney sections were obtained from

nephrectomy specimens, and the cortex was dissected. Isolated glomeruli were cultured for 8 days. After the outgrowing cells were trypsinized and passed through serial sieves, the cells were washed twice with phosphate-buffered saline (PBS). The cultured cells were incubated with Fc receptor blocking reagent (1 µg/mL, BD Bioscience). Podocyte identification was performed by using PE—conjugated rabbit anti-human purified anti-podocalyxin (R&D Systems). The purity of the sorted cells was 98.1%. The media consisted of DMEM/F12 (Lonza) supplemented with 15% FBS (Gibco), 1 × insulin-transferrin-selenium (Gibco), 10 mmol HEPES buffer (Sigma-Aldrich), 200 µmol L-glutamine (Gibco), 50 nmol hydrocortisone (Sigma-Aldrich), 100 U/mL penicillin (Gibco) and 100 pg/mL streptomycin (Gibco) and was changed every 3 days. To determine the optimal media, the media was supplemented in some experiments with 2% or 15% FBS. Plating was routinely performed on plastic dishes coated with 10 µg/mL fibronectin (Sigma-Aldrich). The expression of podocalyxin and PLA2R were assessed by flow cytometry.

## Purification of Immunoglobulin G

To obtain human purified IgG from PLA2R-associated MN patients, serum samples were obtained from PLA2R-associated MN patients (anti-PLA2R level: MN1 [342.3 RU/mL], MN2 [125.7 RU/mL], MN3 [89.7 RU/mL]), a non-PLA2R-associated MN patient (anti-PLA2R

level: MN4 [0.642 RU/mL]), and a healthy control (Con-IgG).

IgG affinity columns were used (Young In frontier) for the purification of IgG. The column was filled with Protein A resin (GE Healthcare) twice the volume of the serum to be used, and then washed with binding buffer. After the column was washed with PBS, the human serum was loaded to a column and reacted with Protein A resin at 4°C for 15 min using a rotator. The column was washed with PBS, and then the elution buffer with 0.1 M citric acid was added. After the elution, the samples were neutralized with 1 M Tris (Thermo Fisher Scientific). The bottom of the sample was removed and the flowthrough was collected. This elution procedure was repeated until $5^{th}$ elution and the collected sample from the individual elution was analyzed. The elution was concentrated using the Centricon centrifugal filter, and PBS was used to dialysis the concentrated elution. After the collection of antibody, the concentration of the antibody was estimated by measuring the optical density at 280 nm by UV spectrophotometer (Biochrom Libra S22). The concentration of purified IgG was calculated by the absorbance × dilution fold/1.36. The purity of purified IgG was analyzed by SDS-PAGE.


# Western blots

To detect the PLA2R band by western blotting of podocyte lysate proteins with IgG from a patient with PLA2R-associated MN

(MN-IgG) or from a healthy control (Con-IgG), equal amounts of podocyte lysate proteins were prepared. The samples were prepared by adding 5×SDS-PAGE loading buffer (Thermo Fisher Scientific) to three volumes of sample and boiling for 5 min at 97℃, as previously described.[1]

Then, the proteins were separated by 6% SDS-PAGE and transferred to Immobilon-FL 0.4-µM polyvinylidene difluoride membranes (Millipore). The membranes were incubated for 1 hr at room temperature in 5% blocking buffer containing 2% bovine serum albumin, and MN-IgG was initially used at a dilution of 1:100 as the primary antibody. Sheep anti-human IgG4 (1:3000, The Binding Site) antibodies were used as a secondary antibody, followed by peroxidase—conjugated donkey anti-sheep IgG (MyBioSource) antibodies as the detecting antibody. At a dilution of 1:2000 for MN-IgG, a band detected at 153 kDa confirmed the location of the PLA2R band. A goat polyclonal antibody against PLA2R (1:200, Novus Biologicals) was used to verify the location of the PLA2R band. The concentration of MN-IgG was serially increased; Con-IgG was loaded as a negative control. The PLA2R band was identified by western blotting of podocyte lysate proteins with IgG isolated from patients with PLA2R antibody-positive MN (n = 3) or from a patient with PLA2R antibody-negative MN (n = 1). To detect the expression of Wilms' tumor 1 (WT1), Snail, fibronectin, and ZO-1, protein was extracted from primary cultured human podocytes using RIPA buffer containing Halt protease inhibitor (Thermo Fisher Scientific). Western

blotting was performed using primary antibodies against fumarate hydratase (1:200, Lifespan Bioscience), Snail (1:50, Abcam), fibronectin (1:100, Santa Cruz Biotechnology), WT1 (1:100, Santa Cruz Biochemistry), ZO-1 (1:200, Invitrogen), and $\beta$-actin (1:20000, Sigma-Aldrich). IgG (1:3000-1:5000, Cell Signaling Technology) was used as a secondary antibody. Approximately 30-50 µg of the extracted protein was separated by 6-10% SDS-PAGE and transferred to Immobilon-FL 0.4-µM polyvinylidene difluoride membranes (Millipore). The western blots shown were representative of four independent experiments. The intensities of the immunoblot band were visualized and captured using an Image Quant LAS 4000 mini (GE Healthcare). Quantification of the western blotting results was performed using ImageJ (National Institutes of Health).

## Immunofluorescence analysis

For immunofluorescence staining of fumarate hydratase in the glomerular section, paraffin-embedded kidney tissue sections from patients with PLA2R-associated MN (n = 5), MCD (n = 5), diabetic nephropathy (n = 5), and non-PLA2R/THSD7A-associated MN (n = 5) were obtained. Normal kidney tissue sections were obtained from histologically normal kidney tissue from kidney donation candidates who underwent kidney biopsy due to asymptomatic urinary abnormalities (n = 5). For immunofluorescence staining for fumarate hydratase in the tubular section, normal kidney tissue from

nephrectomy sample was used. These kidney biopsy specimens provided by National Biobank of Korea (IRB no. 1004-037-315). Antigen retrieval was performed by boiling the samples in citrate buffer at pH 6.1 (30 min at a constant 98°C). Nonspecific binding was blocked with 5% goat serum (Vector Laboratories) with 0.05% Triton-100 (Sigma-Aldrich) in PBS (pH 7.4) for 30 min at room temperature prior to incubation at 4°C overnight with podocalyxin (mouse anti-human, 1:50, Invitrogen) and fumarate hydratase (rabbit anti-human, 1:100, MyBioSource) in blocking buffer. Staining was visualized with Alexa 488—and 555—conjugated probes (Invitrogen) as the secondary antibody.

For the immunofluorescence analysis of ZO-1 expression in primary cultured human podocytes, podocytes were washed with PBS and fixed in 4% formaldehyde for 20 min on ice. The cells were permeabilized with 0.03% Triton X and stained with an antibody against ZO-1 (Invitrogen) in a blocking agent overnight at 4°C, followed by Alexa 555—conjugated probes (Invitrogen). DAPI (Invitrogen) was used to counterstain the nuclei. The primary antibodies were omitted in the negative controls. Immunofluorescence images were acquired by confocal microscopy with a Leica TCS SP8, STED CW system (Leica). The fluorescent intensities of ZO-1 were quantified by MetaMorph software version 7.8.10 (Universal Imaging). The immunofluorescence of fumarate hydratase in the tubules in kidney sections was also measured by MetaMorph software version 7.8.10 (Universal Imaging). These values were corrected by intensity

of immunofluorescence in the specimen of control kidney.


## Lentivirus-mediated fumarate hydratase overexpression

To overexpress fumarate hydratase in primary cultured human podocytes, fumarate hydratase lentiviral activation particles (Santa Cruz Biotechnology) was used as described in the manufacturer's instructions. On day 1, $1.5 \times 10^5$ primary cultured human podocytes was seeded in 2 mL of standard growth medium per well in a six-well tissue culture plate (NUNC A/S) 24 hrs prior to transfection. The cells were grown to 60-80% confluence. On day 2, after a mixture of complete medium with Polybrene (Santa Cruz Biotechnology) at a final concentration of 5 μg/mL was prepared, the media was removed from the wells and replaced with 1 mL of the Polybrene mixture. Thawed lentiviral activation particles were kept on ice. GFP control lentiviral particles (Santa Cruz Biotechnology) were used to measure the transduction efficiency on day 2. On day 3, after the culture medium was removed, 1 mL of complete medium (without Polybrene) was added to each well, and the primary cultured human podocytes were incubated overnight. On day 4, the primary cultured human podocytes were treated with purified IgG from a PLA2R-associated MN patient.

## Intracellular reactive oxygen species assay

Intracellular ROS were determined using an OxiSelect Intracellular ROS assay kit (Cell Biolabs). Cell-permeable fluorogenic 2',7'-dichlorodihydrofluorescein diacetate (DCFH-DA) diffuses into cells and is rapidly oxidized to highly fluorescent 2',7'-dichlorodihydrofluorescein (DCF) by ROS. Primary cultured human podocytes were seeded at $3 \times 10^4$ per well in 96-well plates. At 24 hrs after cell seeding, the cells were treated with Con-IgG, MN-IgG, or MN-IgG after lentiviral fumarate hydratase transduction or MN-IgG after fumarate hydratase siRNA. Cells were washed with PBS and then incubated with 100 μL DCFH-DA/media solution for 30 min at 37°C. The fluorescence intensity of DCFH-DA was measured using a microplate fluorometer (Molecular Devices) with excitation at 485 nm and emission at 530 nm.

## Inhibition of $H_2O_2$-induced ROS generation by apocynin in the podocytes

For identification of the expression of fumarate hydratase and ZO-1 followed by ROS species, primary cultured human podocytes were treated with 1 mM $H_2O_2$ for 24 hrs. The expression levels of fumarate hydratase and ZO-1 were determined in the podocytes treated with apocynin (Sigma-Aldrich) at the indicated concentrations 1 hr before treatment with $H_2O_2$.

## Assembly of C5b-9 on the podocytes *in vitro*

The purified human complement components C5b-6, C7, C8, and C9 (Complement Technologies) were used to assemble C5b-9 in the podocytes.[22] Preincubation of C5b-6 (0.8 μg/mL) was performed at 37°C for 15 min, and C7, C8, and C9 at 10 μg/mL each were further added and incubated with the podocytes for 30 min. The podocytes were washed with serum-free medium to remove excess non-complexed complement components and incubated with 2% FBS for 24 hrs. The formation of C5b-9 on the membrane of the podocytes was identified by confocal microscopy after a 3-hr treatment with C5b-9.

## Fumarate hydratase inhibition induced by siRNA transfection

For inhibition of the fumarate hydratase activity in primary cultured human podocytes, siRNA was transfected targeting fumarate hydratase (Santa Cruz Biotechnology) as described in the manufacturer's protocol. $2 \times 10^5$ primary cultured human podocytes were seeded per well (NUNC A/S) in 2 mL of antibiotic-free normal growth medium supplemented with FBS for 24 hrs prior to transfection. The cells were grown to 60‒80% confluence at 37°C in a $CO_2$ incubator. The siRNA duplex solution was diluted with the transfection reagent. After 24 hrs of fumarate hydratase siRNA

transfection, the primary cultured human podocytes were treated with MN-IgG.

## Immunoprecipitation

Immunoprecipitation followed by immunoblotting was performed to detect the anti-fumarate hydratase autoantibody in the serum of the patients with PLA2R-associated MN (n = 3) and non-PLA2R-associated MN (n = 3) and the healthy controls (n = 3). The serum samples were diluted with 500 µL of immunoprecipitation solution (1:5,000, 1:10,000, GE Healthcare). Then, 50 µL of Protein G Sepharose 4 Fast Flow resin (GE Healthcare) was added and incubated at 4°C overnight, and the samples were centrifuged at 13,000 g force for 2 min. After the samples were washed four times with cold Tris-buffered saline with Tween 20 (Thermo Fisher Scientific), the remaining supernatants were concentrated. SDS-gel electrophoresis loading buffer was added to the beads and supernatants, and the samples were boiled for 5 min at 95°C. Western blotting was performed using primary antibodies against fumarate hydratase (1:1,000, LS Bioscience). Anti-mouse IgG (1:5,000, Cell Signaling Technology) was used as a secondary antibody. For detection of the fumarate hydratase band (predicted molecular weight 55 kDa) as an autoantigen, recombinant human fumarate hydratase (RayBiotech) was used for immunoblotting.

# Enzyme-linked immunosorbent assay

Recombinant human fumarate hydratase (RayBiotech, 1 μg/mL) in 0.05 mM carbohydrate buffer was incubated in a 96-well plate (Thermo Fisher Scientific) overnight at 4°C. The plates were washed three times and blocked in 2% BSA in phosphate-buffered saline with Tween 20 at 37°C for 3 hrs. The wells were then incubated with the serum (1:5,000 and 1:10,000 diluted in 100 μL in each well) from the patients with PLA2R-associated MN (n = 3) and non-PLA2R-associated MN (n = 3) and the healthy controls (n = 3) at room temperature for 1 hr. The plates were washed three times with phosphate-buffered saline with Tween 20. Anti-human IgG antibody (1:1,000, Abcam) and anti-fumarate hydratase antibody (LS Bioscience, 2.5 μg/mL) for the positive control were incubated in the well at room temperature for 1 hr. After the samples were washed, HRP-labeled anti-mouse IgG secondary antibody (1:3,000, Abcam) was added to the wells and incubated for 30 min at room temperature. After further washes, 50 μL of ortho- phenylenediamine in phosphocitrate buffer was added to the well. The reaction was stopped by addition of 50 μL of 2 N sulfuric acid to the wells. The absorbance was read at 450 nm.

# Liquid chromatography (LC)-mass spectrometry (MS)

Fumarate was extracted from cells with a solvent composed of methanol, distilled water, and chloroform. Samples were centrifuged at 7000 g force for 10 min at 4°C. Then, the supernatant of the organic phase was transferred to a new tube and dried under vacuum. Dry residues of extracts were dissolved in 50 µL of distilled water. To quantify the level of fumarate in the cells, liquid chromatography (LC)-mass spectrometry (MS) was performed on an Agilent 1290 Infinity LC and an Agilent 6495 Triple Quadrupole MS system equipped with an Agilent Jet Stream electrospray ionization (ESI) source (Agilent Technologies). MassHunter Workstation (Version B.06.00, Agilent Technologies) software was used for data acquisition and processing. LC separation was carried out on a Scherzo SM-C18 column (100 × 2 mm, particle size 3 µm, Imtakt) in reverse-phase mode for 14 min. The column temperature and flow rate were set to 25°C and 0.4 mL/min, respectively. The mobile phases used were 0.1% formic acid in water (A) and methanol (B). The linear gradients were as follows: 5% B for 3 min; 5-30% B for 3 min; 30-100% B for 5 min; 100% B for 2 min; 100-5% B for 1 min; and 5% B for 3 min. LC-MS/MS experiments were conducted in negative-ion mode with the following parameters: drying gas temperature, 120°C; drying gas flow rate, 11 L/min; nebulizer gas, nitrogen at 40 psi; sheath gas temperature, 350°C; sheath gas flow rate, 12 L/min; capillary voltage, 4 kV; and nozzle voltage, 500 V. Quantification was performed in selected reaction monitoring (SRM) mode, and the SRM parameters were optimized with standard compound solution (1 µg/mL). The

SRM transition of m/z 115→71 was used with a collision energy of 4 V.

## Albumin-rhodamine transit assay

For the albumin-rhodamine transit assay, primary cultured human podocytes were placed onto a Transwell system in 24-well plates (NUNC A/S) with 0.4 μm pore membranes in DMEM/F12 (Invitrogen). Albumin-rhodamine (Abcam) suspended in DMEM/F12 was added to the podocyte monolayer. The transition rate of albumin-rhodamine across the monolayer was assessed by measuring the increase in albumin-rhodamine in the lower well 24 hrs later. Quantification was performed using a standard curve for albumin-rhodamine with a spectrophotometer at an excitation wavelength of 550 nm and an emission wavelength of 570 nm.

## Statistical analysis

Quantitative analysis for western blots was presented as the mean ± standard error of the mean and these were obtained by using Prism (GraphPad Software, Inc.). A one-way analysis of variance followed by Bonferroni *post-hoc* test for comparisons between the groups. Statistical analyses were performed using Statistical Package for the Social Sciences (version 25). A $p$-value $< 0.05$ was considered significant.

# Results

## Glomerular expression of fumarate hydratase in PLA2R-associated MN

First, the expression of fumarate hydratase, which catalyzes the conversion of fumarate to malate, was investigated in the kidney specimens of PLA2R-associated MN patients compared with control, patients with non-PLA2R/THSD7A-associated MN, diabetic nephropathy, and MCD. The results of PLA2R staining was defined as positive[23] if PLA2R staining was distributed along the glomerular capillary loops in a fine granular pattern and colocalized with IgG4 (Figure 1).

Figure 1.
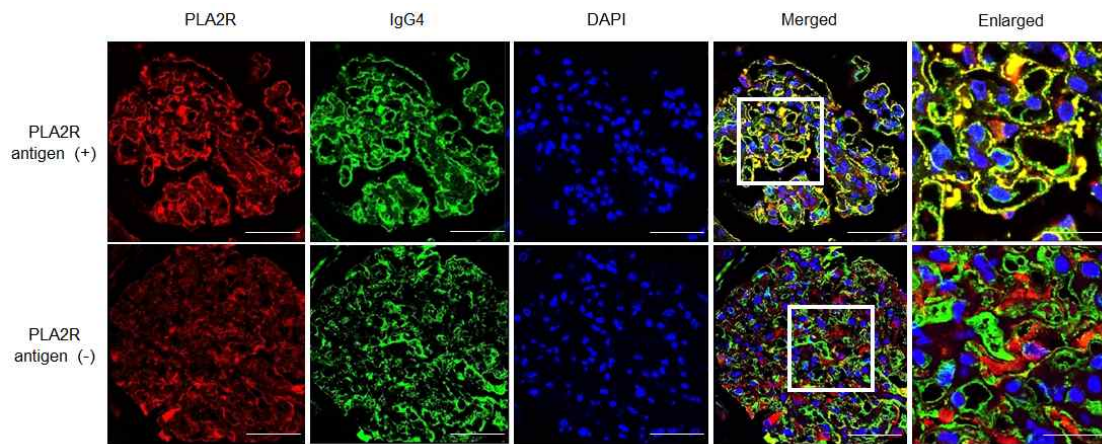


Representative confocal microscopic images of PLA2R antigen-positive and PLA2R antigen-negative kidney specimens. Original magnification × 600. Scale bars: 50 ㎛ (enlarged: × 1,600, Scale bars: 20 ㎛). PLA2R, phospholipase A2 receptor; DAPI; 4'-6-diamidino-2-phenylindole.

Fumarate hydratase colocalized with podocalyxin in the control glomeruli, indicating that podocytes were main cell responsible for the expression of fumarate hydratase. The intensity of fumarate hydratase immunofluorescence and its colocalization signal with podocalyxin were lower in kidney sections from PLA2R-associated MN and diabetic nephropathy patients, which were used as a positive control based on a previous report[15], than in those from the controls, non-PLA2R/THSD7A-associated MN, and MCD patients (Figure 2).

Figure 2.
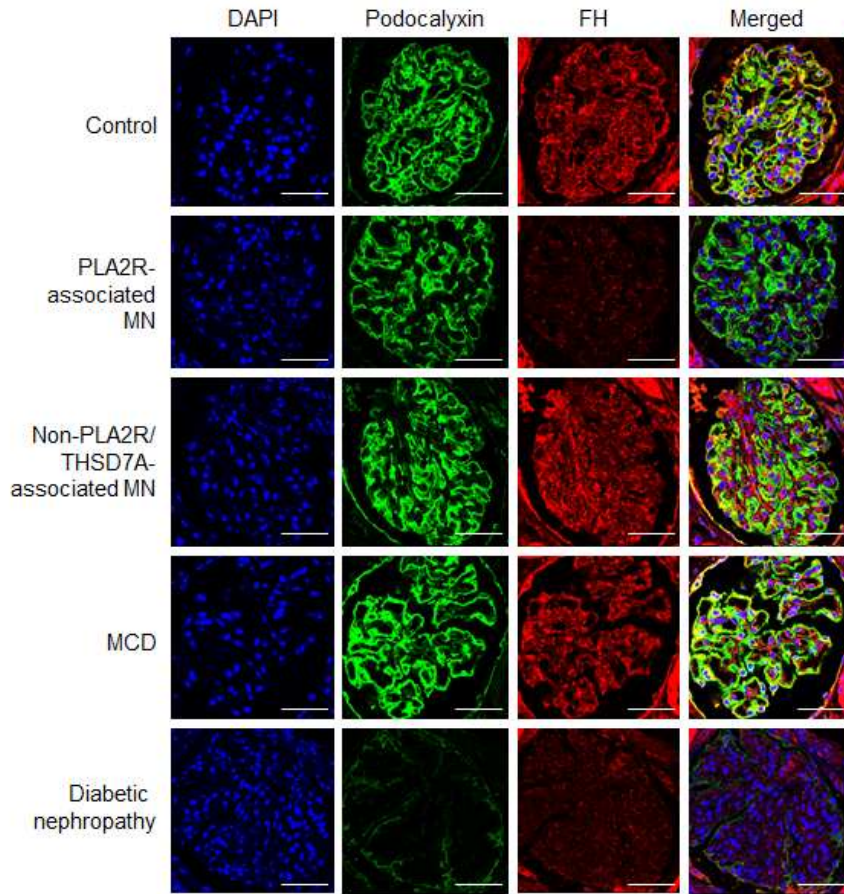


Representative confocal microscopy images of DAPI (blue), podocalyxin (green), and fumarate hydratase (red) staining, along with merged images of kidney sections from controls and patients with PLA2R-associated MN, non-PLA2R/THSD7A-associated MN, MCD, and diabetic nephropathy. Original magnification × 600. Scale bars: 50 μm.

FH, fumarate hydratase; PLA2R, phospholipase A2 receptor; MN, membranous nephropathy; THSD7A, thrombospondin type I domain-containing 7A; MCD, minimal change disease.

There were no significant differences in the tubular expression of fumarate hydratase between kidney sections from PLA2R-associated MN patients and those from MCD patients or controls, although it was decreased in sections from diabetic nephropathy patients (Figure 3A and B).

Figure 3.
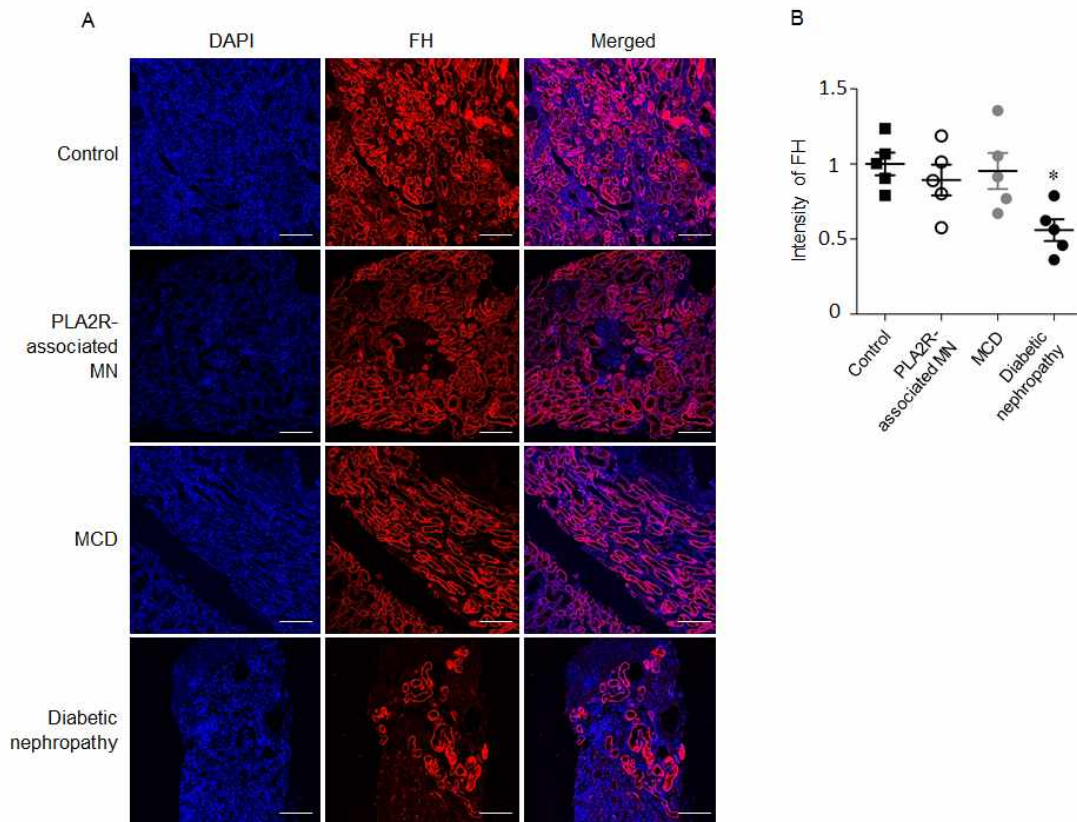


(A) Representative confocal microscopy images of DAPI (blue), fumarate hydratase (red), and merged images of tubules in kidney sections from patients who underwent nephrectomy because of renal cell carcinoma (Control), patients with PLA2R-associated MN, MCD, and diabetic nephropathy. Original magnification × 100. Scale bars: 200 μm.

(B) Relative quantification of the intensity of fumarate hydratase in the tubules of kidney sections from patients who underwent nephrectomy because of renal cell carcinoma (Control), patients with PLA2R-associated MN, MCD, and diabetic nephropathy. $^*p < 0.05$ *vs.*

Control group.

FH, fumarate hydratase; PLA2R, phospholipase A2 receptor; MN, membranous nephropathy; MCD, minimal change disease.

## *In vitro* experiment using purified IgG from a PLA2R-associated MN patient

According to the study identified the anti-PLA2R autoantibody using human glomerular extracts and with serum containing IgG recognized PLA2R antigen,[1] the present study used the purified IgG from patients with PLA2R-associated MN. To elucidate the role of fumarate in podocyte injury caused by the PLA2R antigen-antibody reaction, IgG fractions was purified from serum samples from PLA2R-associated MN patients (anti-PLA2R level: MN1 [342.3 RU/mL], MN2 [125.7 RU/mL], MN3 [89.7 RU/mL]), a non-PLA2R-associated MN patient (anti-PLA2R level: MN4 [0.642 RU/mL]), and a healthy control (Con-IgG). To test whether the PLA2R antigen-antibody reaction could occur in the *in vitro* model, the purified IgG was used to immunoblot the lysates of primary cultured human podocytes at concentrations of 25, 50, 100, and 200 μg/mL. The MN-IgG along with the commercial anti-PLA2R demonstrated bands at 153 kDa, and its intensity increased in a dose-dependent manner; however, the PLA2R antibody-negative MN-IgG or Con-IgG did not (Figure 4), indicating that the MN-IgG from PLA2R antibody-positive patients, but not the Con-IgG, reacted with PLA2R protein from the primary cultured human podocytes. Therefore, further *in vitro* experiments mimicking PLA2R-associated MN milieu were performed using MN-IgG from MN1 patient.

Figure 4.
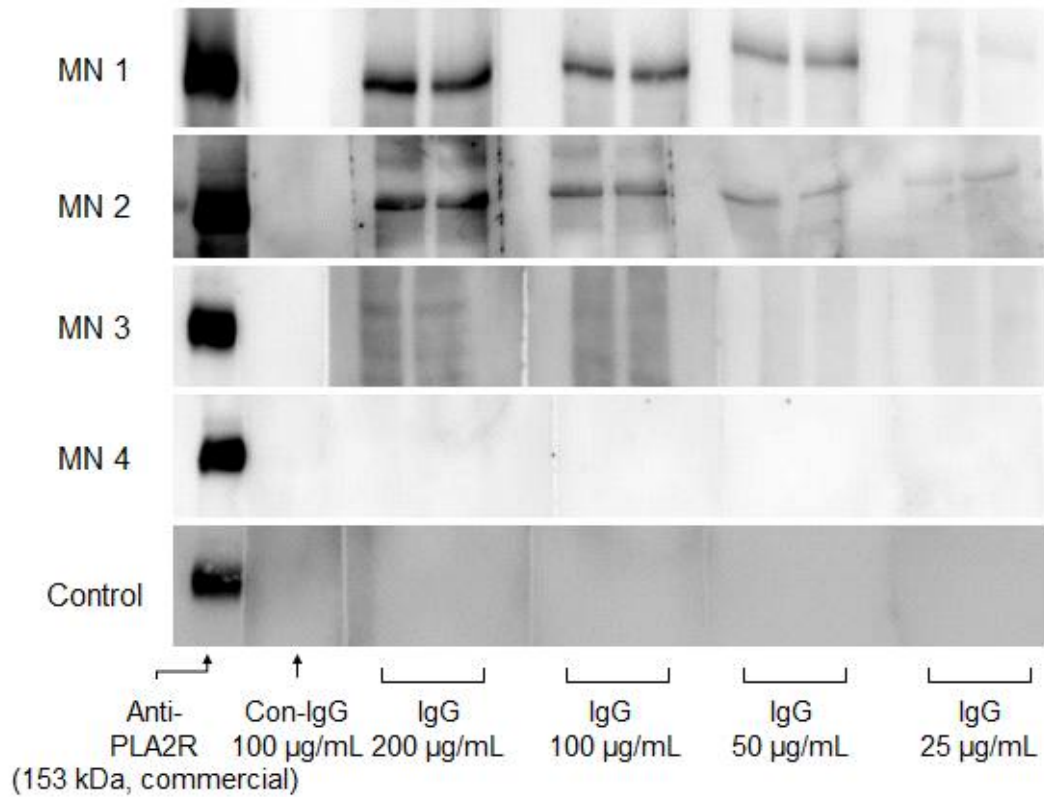


Representative western blots of lysate proteins extracted from primary cultured human podocytes treated with a commercial polyclonal antibody against PLA2R or purified IgG from each of three patients with PLA2R-associated MN (anti-PLA2R level: MN1, 342.3 RU/mL; MN2, 125.7 RU/mL; MN3, 89.7 RU/mL), one patient with non-PLA2R-associated MN (anti-PLA2R level: MN4, 0.642 RU/mL) and one healthy control (Control).

PLA2R, phospholipase A2 receptor; MN, membranous nephropathy.

# Effect of MN-IgG on fumarate hydratase and markers of podocyte phenotype

To examine the role of the MN milieu in podocyte injury, the impact of MN-IgG on the expression of markers of the podocyte phenotype was investigated. Primary cultured human podocytes treated with MN-IgG, but not with Con-IgG, showed a dose-dependent decrease in fumarate hydratase expression (Figure 5A-C). The expression of ZO-1 and WT1, representing the filtration barrier and podocyte differentiation, respectively, was then assessed.[24] The expression of Snail and fibronectin, the key factors involved in phenotypic profile conversion were also evaluated.[25] The MN-IgG treatment significantly decreased the expression of WT1 and ZO-1 and increased the expression of Snail and fibronectin in podocytes (Figure 5A-C). The ratio of the fumarate level, as assessed by liquid chromatography-mass spectrometry (LC-MS), in podocytes treated with MN-IgG to that in podocytes treated with Con-IgG at the same concentrations increased in a dose-dependent manner (Figure 5D). The intracellular ROS levels were significantly higher in the podocytes treated with MN-IgG than in those treated with Con-IgG at the same concentrations (Figure 5E).

Figure 5.

**A**



| | | | | | |
|---|---|---|---|---|---|
| FH | | | | | |
| WT1 | | | | | |
| Snail | | | | | |
| Fibronectin | | | | | |
| ZO-1 | | | | | |
| β-actin | Vehicle | Con-IgG 25 μg/mL | Con-IgG 50 μg/mL | Con-IgG 100 μg/mL | Con-IgG 200 μg/mL |

**B**



| | | | | | |
|---|---|---|---|---|---|
| FH | | | | | |
| WT1 | | | | | |
| Snail | | | | | |
| Fibronectin | | | | | |
| ZO-1 | | | | | |
| β-actin | Vehicle | MN-IgG 25 μg/mL | MN-IgG 50 μg/mL | MN-IgG 100 μg/mL | MN-IgG 200 μg/mL |

C
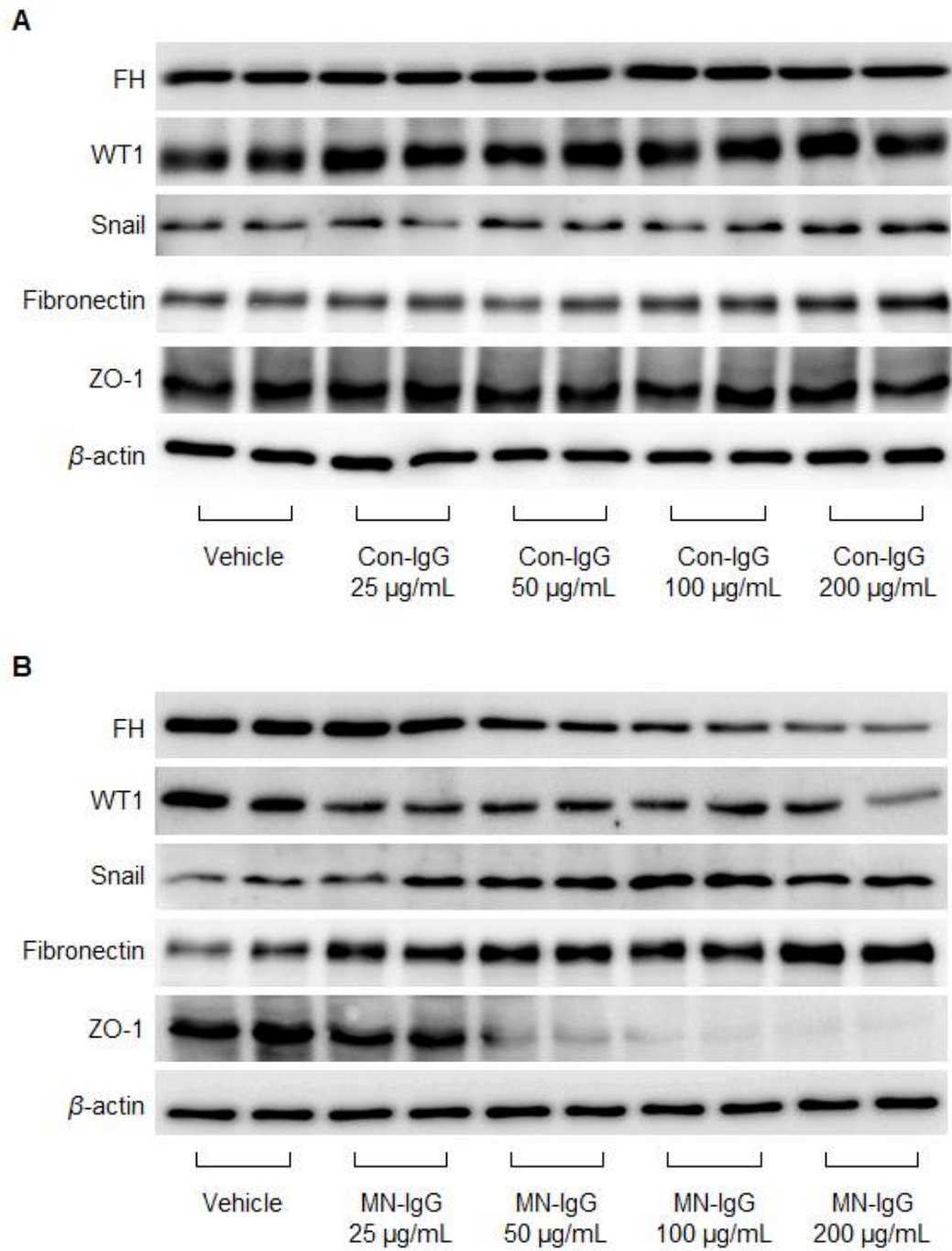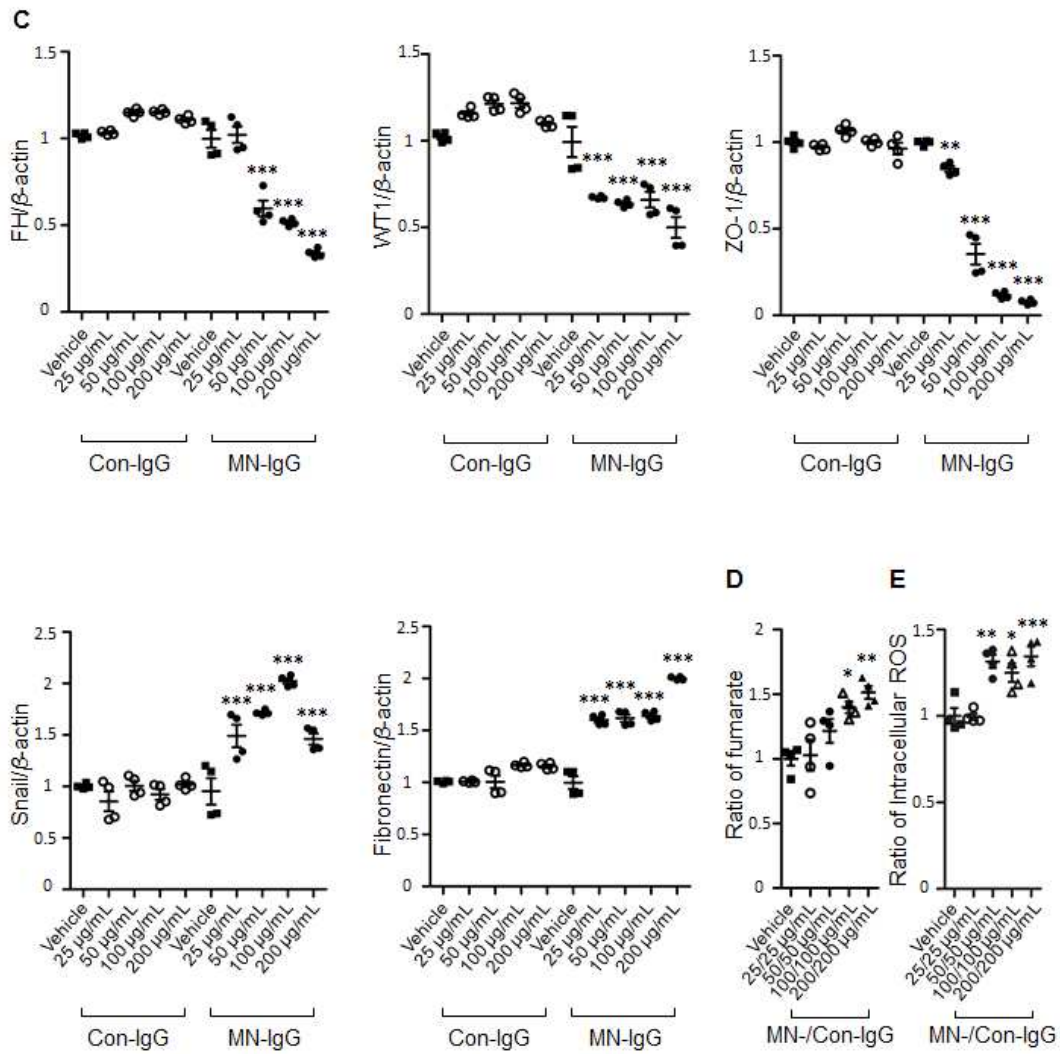
(A-C) Representative western blots (A, B) and densitometric quantification (C) for fumarate hydratase (50 kDa), WT1 (52 kDa), Snail (29 kDa), fibronectin (220 kDa), and ZO-1 (225 kDa) in podocytes after 24 hrs of treatment with Con-IgG (A) or MN-IgG (B).

(D) Liquid chromatography-mass spectrometry analysis of the ratio of the fumarate level in the lysate of MN-IgG-treated podocytes to that of Con-IgG-treated podocytes.

(E) Ratio of the intracellular ROS level in MN-IgG-treated podocytes to that in Con-IgG-treated podocytes.

Data are expressed as the mean ± SEM and were analyzed using one-way analysis of variance followed by the Bonferroni *post hoc* test in (C), (D), and (E).

(C): **$p$-value < 0.01 *vs.* vehicle group, ***$p$-value < 0.001 *vs.* vehicle group.

(D): *$p$-value < 0.05 *vs.* vehicle group, **$p$-value < 0.01 *vs.* vehicle group.

(E): *$p$-value < 0.05 *vs.* vehicle group, **$p$-value < 0.01 *vs.* vehicle group, ***$p$-value < 0.001 *vs.* vehicle group.

FH, fumarate hydratase; MN, membranous nephropathy; WT1, Wilms' tumor 1; ZO-1, zonula occludens-1; ROS, reactive oxygen species.

To investigate whether ROS induced the attenuation of fumarate hydratase, the protein expression levels of fumarate hydratase was measured in the podocytes treated with vehicle or hydrogen peroxide ($H_2O_2$). The $H_2O_2$ treatment attenuated the fumarate hydratase protein expression levels in the podocytes compared with the vehicle treatment (Figure 6A). Pretreatment of apocynin, an NADPH oxidase inhibitor, prevented the $H_2O_2$-induced decrease in fumarate hydratase in a dose-dependent manner (Figure 6A and B). The fumarate hydratase mRNA expression, as assessed by real-time PCR, exhibited a similar pattern as the protein expression (Figure 6C). In addition, the expression of ZO-1 was significantly decreased in the $H_2O_2$-treated podocytes but restored by the apocynin pretreatment (Figure 6B).

Figure 6.
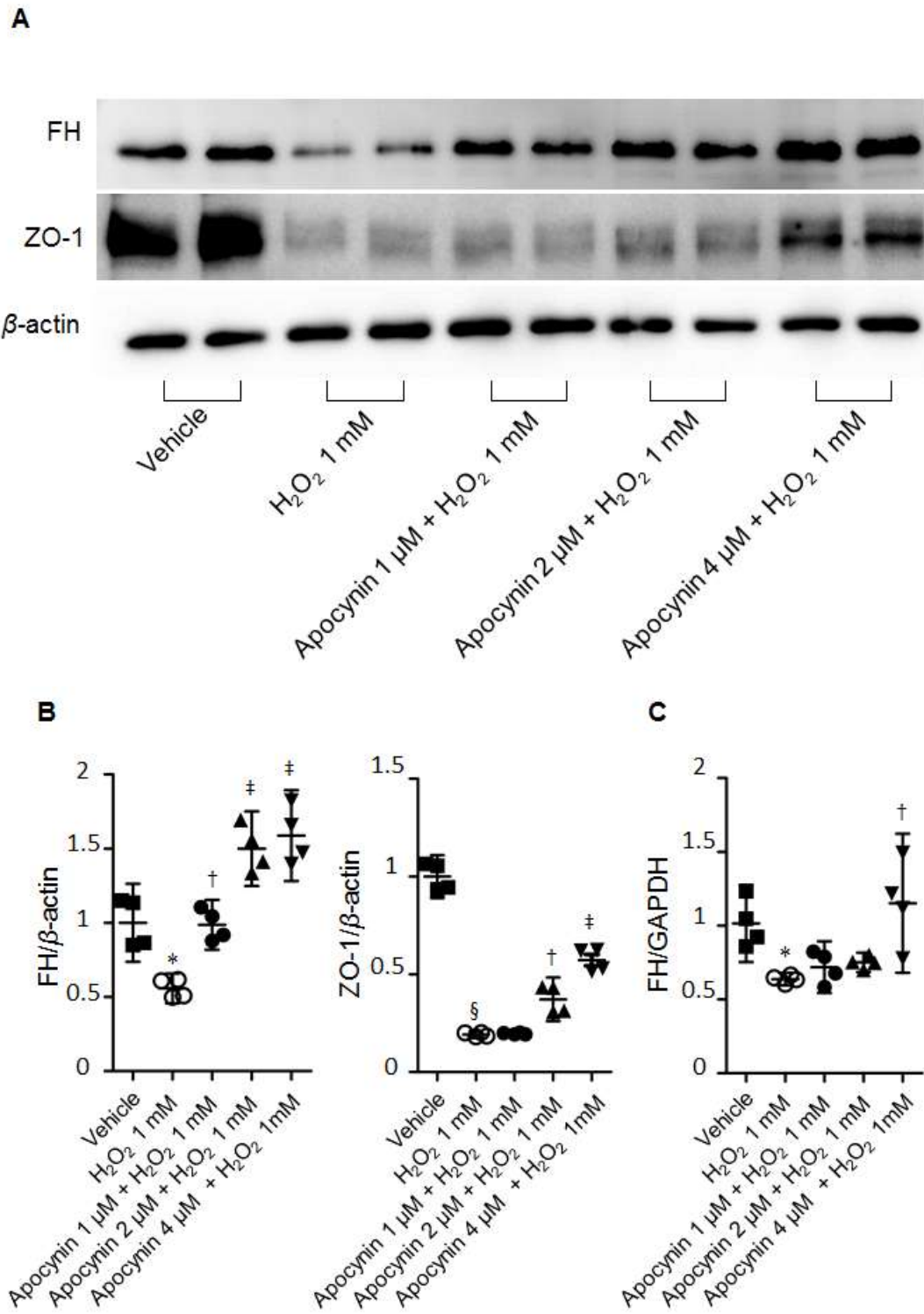
(A, B) Representative western blots (A) and densitometric quantification (B) for fumarate hydratase and ZO-1 in podocytes treated with vehicle, $H_2O_2$ (1 mM), or apocynin (1, 2, or, 4 μM) + $H_2O_2$ (1 mM).

(C) The fumarate hydratase mRNA expression in the podocytes treated with vehicle, $H_2O_2$ (1 mM), or apocynin (1, 2, or, 4 μM) + $H_2O_2$ (1 mM).

Data are expressed as the mean ± SEM and were analyzed using one-way analysis of variance followed by the Bonferroni *post hoc* test in (B) and (C).

(B): $^*p$-value < 0.01 *vs.* vehicle group, $^§p$-value < 0.001 *vs.* vehicle group, $^†p$-value < 0.01 *vs.* $H_2O_2$ (1 mM) treated group, $^‡p$-value <0.001 *vs.* $H_2O_2$ (1 mM) treated group. (C): $^*p$-value < 0.05 *vs.* vehicle group, $^†p$-value < 0.01 *vs.* $H_2O_2$ (1 mM) treated group.

FH, fumarate hydratase; ZO-1, zonula occludens-1; GAPDH: glyceraldehyde 3-phosphate dehydrogenase.

The effect of complement activation on the fumarate hydratase expression in the podocytes was further investigated. The expression of fumarate hydratase in the podocytes treated with the C5b-9 assembly was lower than that in the control podocytes, as shown by confocal microscopy and flow cytometry (Figure 7A-C). These findings suggest that ROS production accompanied by activation of the complement system might participate in the decreased expression of fumarate hydratase in podocytes.

Figure 7.

**A**
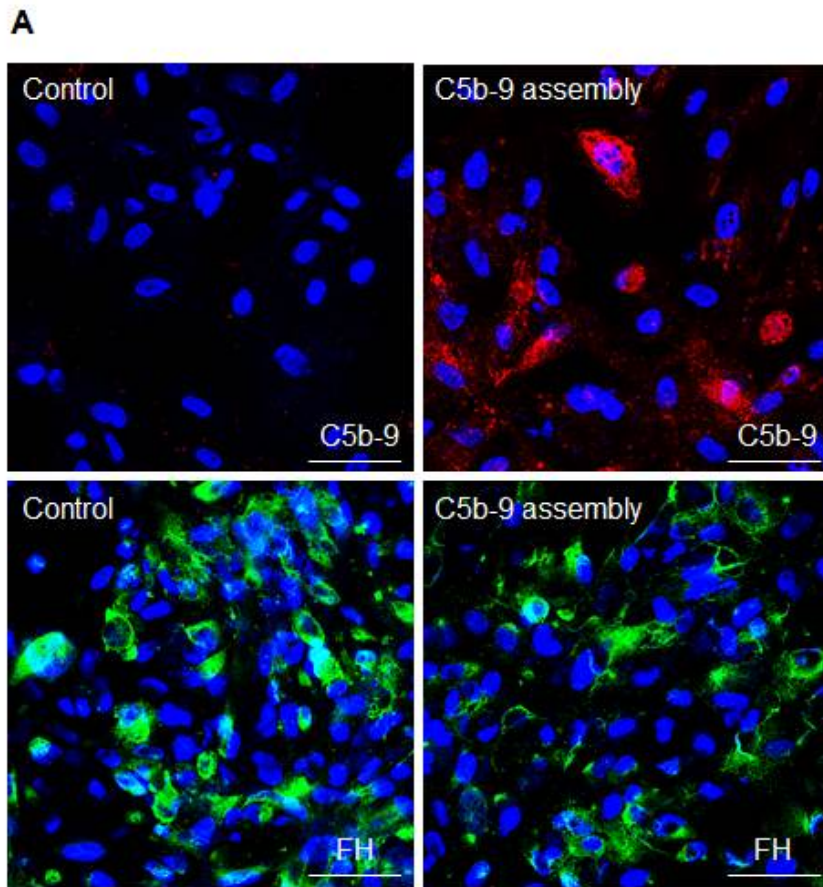


(A) Representative confocal microscopy images of C5b-9 (red, upper panel), fumarate hydratase (green, lower panel), and DAPI (blue) staining in podocytes treated with C5b-9 assembly (right panel) and control podocytes (left panel). Original magnification × 400. Scale bars: 50 μm.

**B**
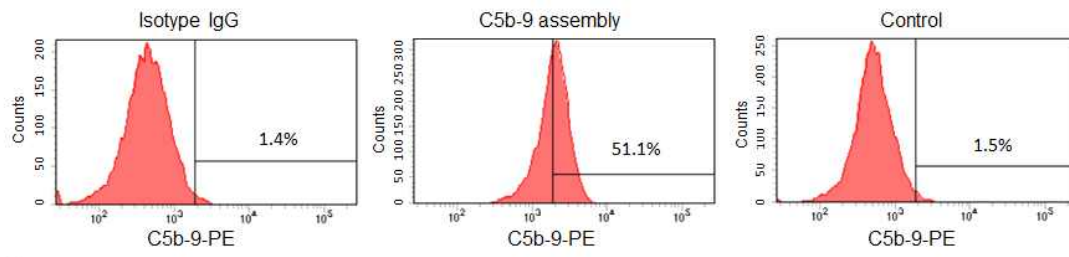


**C**
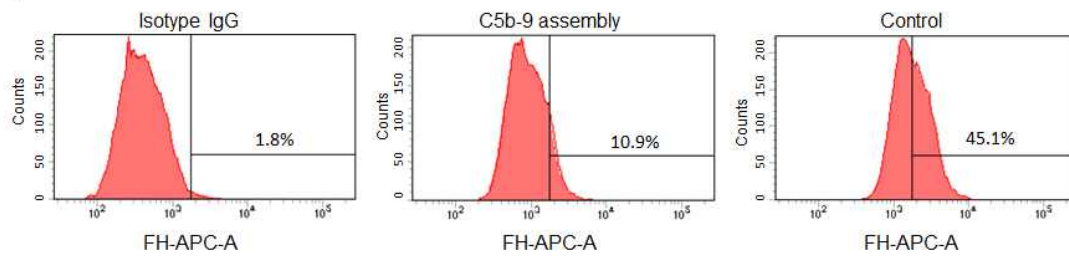


(B, C) Flow cytometry of C5b-9 (B) and fumarate hydratase (C) in podocytes treated with isotype IgG (left), C5b-9 assembly (middle), and control podocytes (right). FH, fumarate hydratase.

The immunoprecipitation analysis as well as enzyme-linked immunosorbent assay (ELISA) were performed to rule out the possibility of anti-fumarate hydratase autoantibody in the sera of the PLA2R-associated MN patients. However, anti-fumarate hydratase autoantibody was not found in the patient serum samples (Figure 8A-D).

Figure 8.
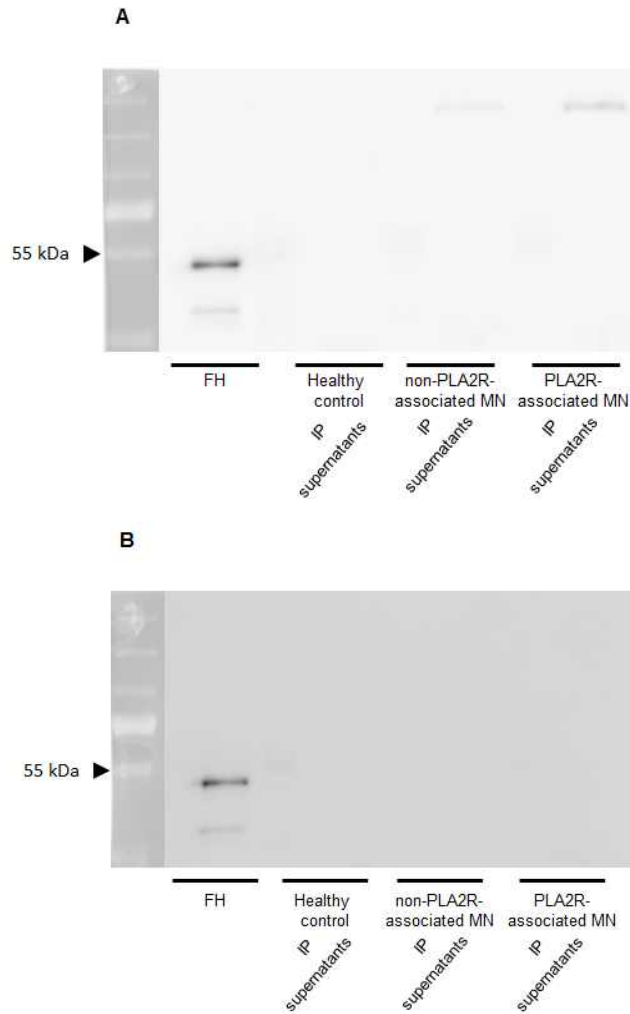


(A, B) Representative images of immunoprecipitation and immunoblot for anti-fumarate hydratase autoantibody in diluted serum samples ((A):1,5,000, (B):1:10,000) from healthy control, patient with non-PLA2R-associated MN, and PLA2R-associated MN. Recombinant human fumarate hydratase was used as a positive control.

FH, fumarate hydratase; IP, immunoprecipitation; PLA2R, phospholipase A2 receptor; MN, membranous nephropathy.
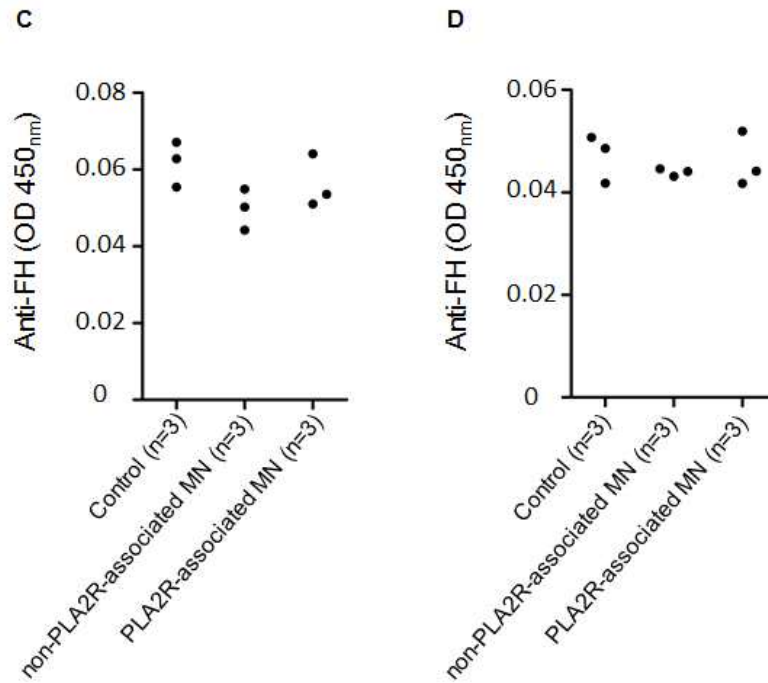
(C, D) Reactivity of serum samples from healthy controls (n = 3), patients with non-PLA2R-associated MN (n = 3), and PLA2R-associated MN (n = 3) against fumarate hydratase determined by enzyme-linked immunosorbent assay. The diluted serum was used ((C):1:5,000, (D): 10,000).

FH, fumarate hydratase; PLA2R, phospholipase A2 receptor; MN, membranous nephropathy; OD, optical density.

Next, the overexpression of fumarate hydratase via the transduction of the cultured podocytes with fumarate hydratase activation lentiviral particles was performed to explore whether the fumarate hydratase overexpression could abrogate these changes. Overexpression of fumarate hydratase using fumarate hydratase activation lentiviral particles significantly increased the endogenous fumarate hydratase protein expression in the cultured podocytes (Figure 9A and B). The fumarate concentration in the lysate of the podocytes, as assessed by LC-MS, was significantly decreased in the treatment of fumarate hydratase activation lentiviral particles-transduced podocytes but not in the control lentiviral particles-transduced cells (Figure 9C).

Figure 9.
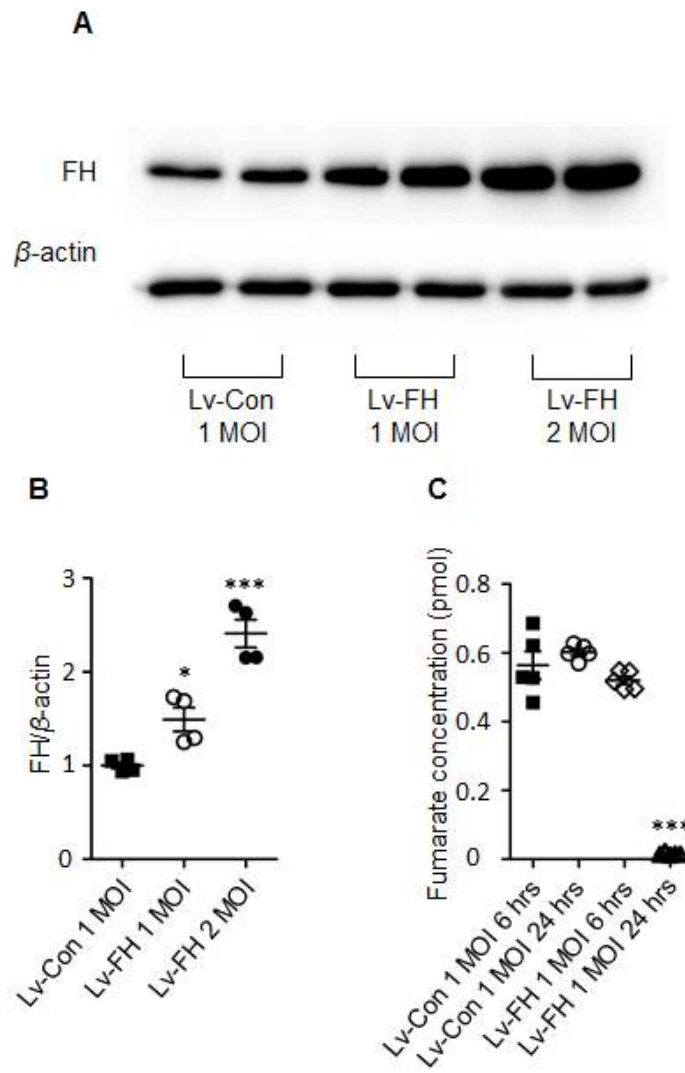
Representative of western blots (A) and densitometric quantification (B) of fumarate hydratase in podocytes transduced with control lentiviral particles at 1 MOI, fumarate hydratase activation lentiviral particles at 1 MOI, or 2 MOI.

(C) Liquid chromatography-mass spectrometry analysis of the fumarate levels in the lysates of podocytes transduced with control lentiviral particles at 1 MOI for 6 hrs, control lentiviral particles at 1 MOI for 24 hrs, fumarate hydratase activation lentiviral particles at 1 MOI for 6 hrs, or fumarate hydratase activation lentiviral particles at 1 MOI for 24 hrs.

Data are expressed as the mean ± SEM and were analyzed using one-way analysis of variance followed by the Bonferroni *post hoc* test in (B) and (C).

(B): $^{*}p$-value < 0.05 *vs.* Lv-Con at 1 MOI group,$^{***}p$-value < 0.001 *vs.* Lv-Con at 1 MOI group.

(C): $^{***}p$-value < 0.001 *vs.* Lv-Con at 1 MOI for 24 hrs group.

FH, fumarate hydratase; Lv-Con, control lentiviral particles; Lv-FH, fumarate hydratase activation lentiviral particles; MOI, multiplicity of infection.

Treatment with MN-IgG significantly increased the expression of Snail and fibronectin and decreased the expression of fumarate hydratase, WT1 and ZO-1, while Con-IgG had no effect. Transduction of fumarate hydratase activation lentiviral particles significantly abrogated the MN-IgG-induced protein expression in the podocytes (Figure 10A and B). The intracellular ROS levels were significantly increased in the podocytes treated with MN-IgG but not in those treated with Con-IgG. Transduction of fumarate hydratase activation lentiviral particles significantly suppressed the intracellular ROS levels compared with those in the podocytes treated with MN-IgG (Figure 10C).

Figure 10.

(A, B) Representative western blots (A) and densitometric quantification (B) of fumarate hydratase, WT1, Snail, fibronectin, and ZO-1 in the podocytes treated with vehicle, fumarate hydratase activation lentiviral particles at 1 MOI, Con-IgG, MN-IgG, or fumarate hydratase activation lentiviral particles at 1 MOI followed by MN-IgG.

(C) Ratio of the intracellular ROS level in the podocytes treated with vehicle, fumarate hydratase activation lentiviral particles at 1 MOI, Con-IgG, MN-IgG, or fumarate hydratase activation lentiviral particles at 1 MOI followed by MN-IgG.

Data are expressed as the mean ± SEM and were analyzed using one-way analysis of variance followed by the Bonferroni *post hoc* test.

(B): $^{§}p$-value < 0.001 *vs.* vehicle group, $^{**}p$-value < 0.01 *vs.* Con-IgG group, $^{***}p$-value < 0.001 *vs.* Con-IgG group, $^{#}p$-value < 0.05 *vs.* MN-IgG group, $^{‡}p$-value < 0.001 *vs.* MN-IgG group.

(C): $^{***}p$-value < 0.001 *vs.* Con-IgG group, $^{‡}p$-value < 0.001 *vs.* MN-IgG group.

FH, fumarate hydratase; Lv-FH, fumarate hydratase activation lentiviral particles; WT1, Wilms' tumor 1; ZO-1, zonula occludens-1; ROS, reactive oxygen species; MN, membranous nephropathy.

To investigate the impact of fumarate hydratase inhibition, cells were transduced with fumarate hydratase siRNA. Fumarate hydratase siRNA alone significantly decreased the expression of WT1 and ZO-1 and increased the intracellular ROS level (Figure 11A, B, and C). Furthermore, treatment with MN-IgG in the fumarate hydratase siRNA-transduced podocytes synergistically decreased the expression of fumarate hydratase accompanied by decreases in WT1 and ZO-1 and increases in fibronectin and Snail (Figure 11A and B).

Figure 11.

(A, B) Representative western blots (A) and densitometric quantification (B) of fumarate hydratase, WT1, Snail, fibronectin, and ZO-1 in the podocytes treated with vehicle, fumarate hydratase siRNA, Con-IgG, MN-IgG, or fumarate hydratase siRNA followed by MN-IgG.

(C) Ratio of the intracellular ROS level in the podocytes treated with vehicle, fumarate hydratase siRNA, Con-IgG, MN-IgG, or fumarate hydratase siRNA followed by MN-IgG.

Data are expressed as the mean ± SEM and were analyzed using one-way analysis of variance followed by the Bonferroni *post hoc* test.

(B): $^{\S}p$-value < 0.001 *vs.* vehicle group, $^{***}p$-value < 0.001 *vs.* Con-IgG group, $^{\#}p$-value < 0.05 *vs.* MN-IgG group, $^{\dagger}p$-value < 0.01 *vs.* MN-IgG group, $^{\ddagger}p$-value < 0.001 *vs.* MN-IgG group.

(C): $^{\S}p$-value < 0.001 *vs.* vehicle group, $^{***}p$-value < 0.001 *vs.* Con-IgG group, $^{\dagger}p$-value < 0.01 *vs.* MN-IgG group.

FH, fumarate hydratase; WT1, Wilms' tumor 1; ZO-1, zonula occludens-1; ROS, reactive oxygen species; MN, membranous nephropathy.

In line with the findings, diethyl fumarate treatment also attenuated the expression of WT1 and ZO-1 in a dose-dependent manner (Figure 12).

Figure 12.
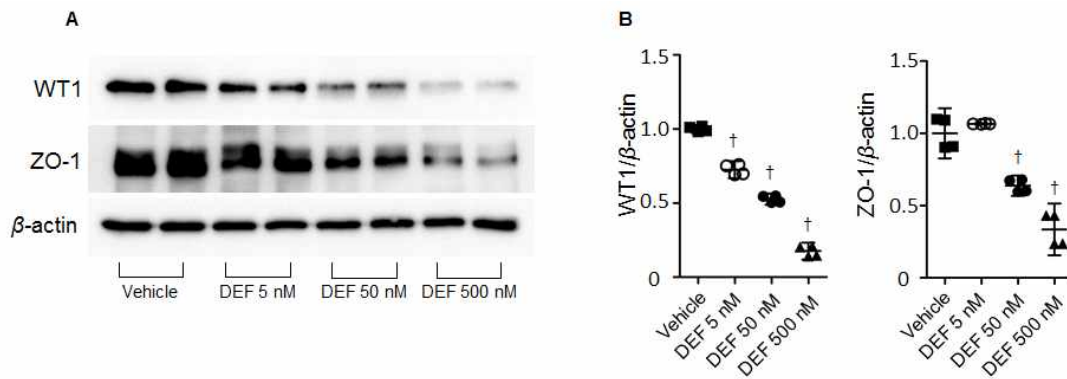


Representative western blot (A) and densitometric quantification (B) of WT1 and ZO-1 in podocytes treated with vehicle, diethyl fumarate (DEF) at 5 nM, 50 nM, or 500 nM.

(B): WT1, $^\dagger p < 0.001$ *vs*. vehicle group; ZO-1, $^\dagger p < 0.001$ *vs*. vehicle group.

FH, fumarate hydratase; WT1, Wilm's tumor 1; ZO-1, zonula occludens-1.

# Effect of fumarate on ZO-1 expression and podocyte permeability to albumin

Because of the dramatic changes in ZO-1 protein expression following MN-IgG treatment, podocytes were stained for ZO-1 to identify cellular lesions responsible for the changes in response to MN-IgG. MN-IgG, but not Con-IgG, decreased the immunofluorescence intensity of ZO-1 in the cultured podocytes, and transducation of fumarate hydratase activation lentiviral particles significantly restored the MN-IgG-induced decrease in ZO-1 immunofluorescence (Figure 13A and B). The albumin-rhodamine transit assay was performed to assess the role of fumarate in the permeability of podocytes to albumin. After 24 hrs of treating podocytes with MN-IgG, the permeability of the podocyte monolayer to albumin was determined. The absorbance of human serum albumin-rhodamine in the media of the lower Transwell chamber was higher after treatment with MN-IgG than with vehicle or Con-IgG. Fumarate hydratase activation lentiviral particles transduction did not completely recover the albumin flux but significantly decreased the MN-IgG-induced increase in the absorbance of human serum albumin-rhodamine (Figure 13C).

Figure 13.

**A**



Vehicle | Con-IgG 50 μg/mL | MN-IgG 50 μg/mL
MN-IgG 100 μg/mL | Lv-FH 1 MOI + MN-IgG 50 μg/mL | Lv-FH 2 MOI + MN-IgG 50 μg/mL

**B**



ZO-1 intensity (Arbitrary units)

**C**



Albumin-rhodamine transit
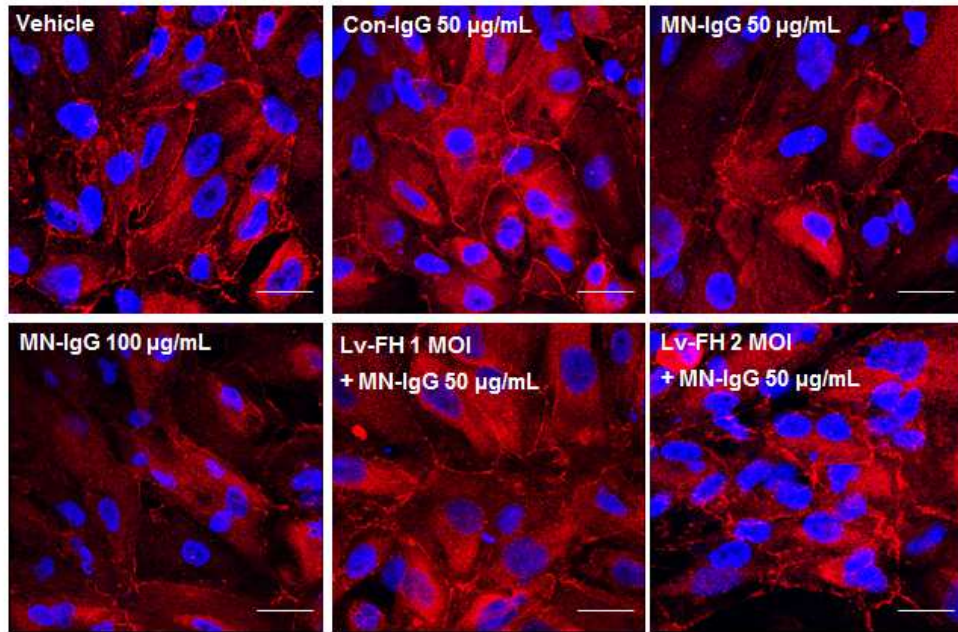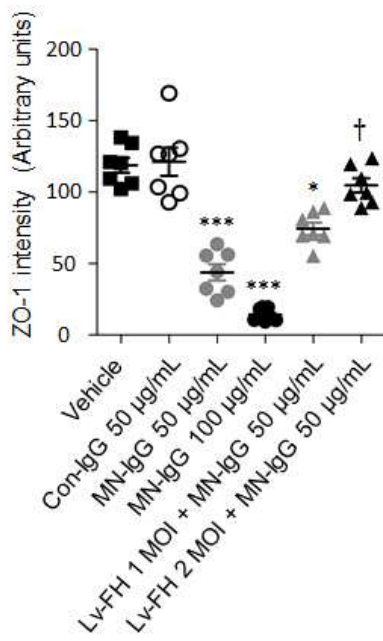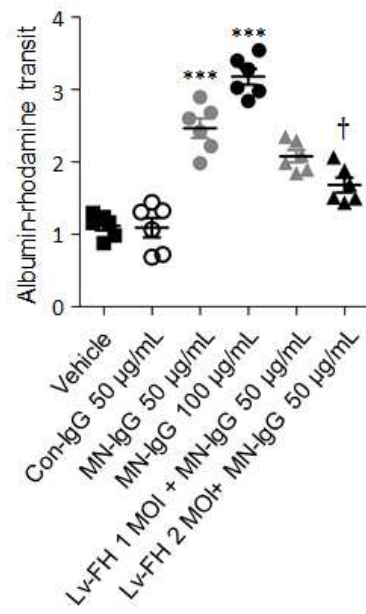
(A, B) Representative confocal microscopy images of ZO-1 (red) and DAPI (blue) staining (A) and fluorescence intensity for ZO-1 (B) in podocytes treated under different conditions: vehicle, Con-IgG 50 µg/mL, MN-IgG 50 µg/mL, MN-IgG 100 µg/mL, fumarate hydratase activation lentiviral particles at 1 MOI followed by MN-IgG 50 µg/mL, fumarate hydratase activation lentiviral particles at 2 MOI followed by MN-IgG 50 µg/mL. Original magnification × 800. Scale bars: 20 µm.

(C) Relative quantification of albumin-rhodamine transit across monolayers of podocytes treated vehicle, Con-IgG 50 µg/mL, MN-IgG 50 µg/mL, MN-IgG 100 µg/mL, or fumarate hydratase activation lentiviral particles at 1 MOI followed by MN-IgG 50 µg/mL and fumarate hydratase activation lentiviral particles at 2 MOI followed by MN-IgG 50 µg/mL.

Data are expressed as mean ± SEM and were analyzed using one-way analysis of variance followed by the Bonferroni *post hoc* test in (B) and (C).

(B): ***$p$-value < 0.001 *vs.* vehicle group, *$p$-value < 0.05 *vs.* MN-IgG 50 µg/mL group, ⁺ $p$-value < 0.001 *vs.* MN-IgG 50 µg/mL group.

(C): ***$p$-value < 0.001 *vs.* vehicle group. ⁺ $p$-value < 0.001 *vs.* MN-IgG 50 µg/mL group.

ZO-1, zonula occludens-1; Lv-FH, fumarate hydratase activation lentiviral particles; MOI, multiplicity of infection.

# Discussion

The pathological mechanism that leads to podocyte injury downstream of PLA2R autoimmunity is clinically important because it might be a potential therapeutic target for MN, given that a significant proportion of patients do not respond to immunosuppressive treatment.[9,10] The podocytes treated with purified IgG from serum with a high anti-PLA2R titer showed decreased fumarate hydratase expression and increased fumarate levels accompanied by phenotypic alteration, ROS stimulation, and increased podocyte permeability to albumin. Interestingly, fumarate hydratase overexpression ameliorated these unfavorable changes, whereas inhibition of fumarate hydratase enhanced these changes. These findings suggest that fumarate plays a role in podocyte injury as a downstream mechanism in the PLA2R antigen-antibody reaction.

 The colocalization of fumarate hydratase with podocyte marker and the marked decrease in its expression in the glomeruli of PLA2R-associated MN patients indicating that podocytes were main cell responsible for the expression of fumarate hydratase. This study demonstrated that the fumarate hydratase levels were decreased in cultured podocytes treated with MN-IgG, which was accompanied by an increase in fumarate. Furthermore, the intensity of fumarate hydratase was decreased in the kidney biopsy sections from the PLA2R-associated MN group but not in those from the non-PLA2R-associated MN group. These data indicate that the

- 55 -

inhibition of fumarate hydratase and subsequent accumulation of fumarate may occur in podocytes following the PLA2R antigen-antibody reaction.

For analysis of the mechanism of how PLA2R autoimmunity attenuates fumarate hydratase, the present study demonstrated that complement activation and ROS production could decrease fumarate hydratase, which is consistent with previous data.[15] Although this study could not show a sequential and direct relationship between PLA2R autoimmunity, complement activation, ROS, and fumarate hydratase in primary cultured human podocytes, an increase in ROS through complement system activation could be a possible mechanism that reduces fumarate hydratase expression. On the contrary, it could be possible that pathological mechanisms other than ROS generation through complement system activation might be involved in non-PLA2R/THSD7A-associated MN, given that the expression of fumarate hydratase was preserved in their kidney specimens. The hydrolysis of fumarate to malate is one of the major reactions in the tricarboxylic acid cycle, and the reaction is catalyzed by fumarate hydratase.[26] Thus, the inactivation of fumarate hydratase results in the intracellular accumulation of fumarate.[27] Based on the importance of this pathway in oxidative phosphorylation, fumarate accumulation affects various signaling pathways, including those involved in cellular endoplasmic reticulum (ER) stress and phenotypic change of podocytes, through the production of ROS.[17,28,29] A recent investigation has suggested that fumarate is associated with all-cause mortality of

chronic kidney disease patients.[30] Fumarate also plays a role in the progression of diabetic nephropathy by stimulating ER stress and extracellular matrix production.[15] These data suggest that fumarate may cause podocyte injury in PLA2R-associated MN.

The surplus of ROS could elicit injurious consequences in renal pathophysiology.[15] Upregulation of ROS produced by NADPH has been known to induce impaired glomerular hemodynamics.[31] It has been also confirmed the attenuated expression of fumarate hydratase by overexpression of NADPH oxidase 4 activity.[15] Decreased expression of glomerular fumarate hydratase and the increased urine fumarate in PLA2R-associated MN patients might be the result of an imbalance between podocyte antioxidant capacity and overproduction of oxidative stress in the PLA2R-associated MN disease entity. Also, fumarate itself is known to be served to an accumulation of ROS by binding antioxidant glutathione.[28] In accordance with the previous investigation, this study showed that the inhibition of fumarate hydratase activity alone induced an increase of intracellular ROS production in the podocytes. These findings suggest that fumarate could be both of the consequences or the cause of ROS-induced podocyte injury following PLA2R-autoimmunity. In view of this mutual interaction between ROS and fumarate, and the association of renal injury, the therapeutic intervention to fumarate production may have protective effects in podocyte injury. Treatment with NOX4 inhibitor, which can restore the attenuated expression of fumarate hydratase in the diabetic animal model showed the reduction of

albuminuria and fibronectin expression.[15] Also, the therapeutic intervention of this agent has been investigated as a treatment of diabetic nephropathy in humans. This therapeutic intervention that can restore the fumarate hydratase expression in PLA2R-associated MN is expected to prevent podocyte injury and to alleviate proteinuria.

Loss of typical podocyte phenotype is a crucial process in podocyte injury in many glomerular diseases, including MN.[32] During the process of cellular injury, podocytes lose their epithelial features, which is characterized by reduced ZO-1 expression; simultaneously, podocytes acquire mesenchymal features, including increased fibronectin expression.[25,33] These phenotypical changes are further indicated by the fact that the expression of Snail, a prominent inducer of phenotypic profile change, may be induced following the injurious stimulation of podocytes, eventually leading to podocyte dysfunction and albuminuria.[25] A recent study demonstrated that the phenotypic change of podocytes might also be induced by the deletion of WT1,[34] which is required for maintaining the differentiated phenotype during podocyte injury in proteinuric kidney diseases, such as diabetic nephropathy and MN.[35,36] Interestingly, the inhibition of fumarate hydratase activity and the subsequent accumulation of fumarate have been reported to trigger the change of phenotypic profile through the mechanism by which fumarate induces ROS by modifying glutathione metabolism or ROS-related-miRNAs.[28,29,37] The present study demonstrated that the podocytes in the milieu of PLA2R-associated

MN lose their epithelial and differentiation markers accompanied by the acquisition of mesenchymal features. These phenotypic changes developed simultaneously with the dysregulation of fumarate hydratase, and the overexpression of fumarate hydratase might restore the MN-IgG-induced pathological alterations. In contrast, the inhibition of fumarate hydratase enhanced the alteration of phenotypic profile by MN-IgG. These results indicate that fumarate could cause phenotypic changes in podocytes subsequent to the PLA2R antigen-antibody reaction. Furthermore, overexpression of fumarate hydratase attenuated the upregulation of intracellular ROS in response to PLA2R autoimmunity in podocytes. These results were consistent with those of a previous study, which showed a decrease in intracellular ROS by preventing the accumulation of fumarate by blocking the responsible enzymes of the tricyclic acid cycle.[28]

These findings provide insight into the mechanism underlying podocyte injury subsequent to PLA2R autoimmunity through increasing intracellular ROS, and thus suggest that fumarate may be a potential therapeutic target in PLA2R-associated MN. Moreover, phenotypic alterations in podocytes may contribute to functional perturbations in the glomerular filtration barrier. This study observed that the expression of ZO-1, an adaptor protein of the slit diaphragm[38] was suppressed in cell-cell junctions after the PLA2R antigen-antibody reaction. These factors contribute to the impairment of cell-cell junction integrity and subsequently increased permeability to albumin. Interestingly, the overexpression of fumarate hydratase

attenuated the permeability of the podocyte layer to albumin that was induced by MN-IgG stimulation. Collectively, fumarate plays a crucial role in podocyte dysfunction via phenotypic alterations following PLA2R autoimmunity, even though the metabolite may not be exclusively disease-specific for PLA2R-associated MN.

There are several limitations to this study. The present study could not prove the pathological mechanism of fumarate by *in vivo* animal experiments. Instead, *in vitro* podocyte experiments mimicking the milieu of PLA2R-associated MN was performed, in line with a previous study that demonstrated the reaction between serum samples from PLA2R-associated MN patients and human glomerular extracts.[1] Second, the permeability test using cultured podocytes might not be able to evaluate the function of slit diaphragm since cultured podocytes tend to form tight junctions instead of slit diaphragm.[39] Third, the downregulation of fumarate hydratase could be due to other circulating anti-podocyte antibodies that may potentially coexist in the purified IgG from MN patients.[40] In addition, the modulations of the enzyme activity of fumarate hydratase could potentially affect the function of multiple enzymes in the TCA cycle or other pathways by altering the substrates metabolized by these enzymes.[41,42] These alterations could lead to the dysregulation of various signaling pathways for podocyte cellular metabolism. Thus, this study has a limitation that the expression of podocyte injury markers might not have occurred only with the changes in the enzyme activity of fumarate hydratase. In summary, these findings provide evidence of

the role played by fumarate in podocyte injury subsequent to PLA2R-autoimmunity through the acquisition of the mesenchymal phenotype and the loss of cell-cell adhesion and indicate that fumarate may be a potential target for therapeutic intervention in PLA2R-associated MN.

# 참 고 문 헌

1. Beck Jr LH, Bonegio RG, Lambeau G, et al. M-type phospholipase A2 receptor as target antigen in idiopathic membranous nephropathy. N Engl J Med. 2009;361:11-21.

2. Stanescu HC, Arcos-Burgos M, Medlar A, et al. Risk HLA-DQA1 and PLA2R1 alleles in idiopathic membranous nephropathy. N Engl J Med. 2011;364:616-626.

3. Gupta S, Köttgen A, Hoxha E, et al. Genetics of membranous nephropathy. Nephrol Dial Transplant. 2017;33:1493-1502.

4. Marson A, Housley WJ, Hafler DA. Genetic basis of autoimmunity. J Clin Invest. 2015;125:2234-2241.

5. Ruggenenti P, Debiec H, Ruggiero B, et al. Anti-phospholipase A2 receptor antibody titer predicts post-rituximab outcome of membranous nephropathy. J Am Soc Nephrol. 2015;26:2545-2558.

6. Kanigicherla D, Gummadova J, McKenzie EA, et al. Anti-PLA2R antibodies measured by ELISA predict long-term outcome in a prevalent population of patients with idiopathic membranous nephropathy. Kidney Int. 2013;83:940-948.

7. Hoxha E, Harendza S, Pinnschmidt H, et al. M-type phospholipase A2 receptor autoantibodies and renal function in patients with primary membranous nephropathy. Clin J Am Soc Nephrol. 2014;9:1883-1890.

8. Song EJ, Jeong KH, Yang YA, et al. Anti-phospholipase A2 receptor antibody as a prognostic marker in patients with primary membranous nephropathy. Kidney Res Clin Pract. 2018;37:248-256.

9. Fervenza FC, Appel GB, Barbour SJ, et al. Rituximab or cyclosporine in the treatment of membranous nephropathy. N Eng J Med. 2019;381:36-46.

10. Hanset N, Esteve E, Plaisier E, et al. Rituximab in patients with PLA2R-associated membranous nephropathy and severe chronic kidney disease. Kidney Int Rep. 2019;5:331-338.

11. Kerjaschki D, Neale TJ. Molecular mechanisms of glomerular injury in rat experimental membranous nephropathy (Heymann nephritis) J Am Soc Nephrol. 1996;7:2518-2526.

12. Larsen CP, Messias NC, Silva FG, et al. Determination of primary versus secondary membranous nephropathy utilizing phospholipase A2 receptor staining in renal biopsies. Mod Pathol. 2013;26:709-715.

13. Pippi JW, Dursaula R, Petermann A, et al. DNA damage is a

novel response to sublytic complement C5b-9 induced injury in podocytes. J Clin Invest. 2003;111:877-885.

14. Nangaku M, Shankland SJ, Couser WG, et al. Cellular response to injury in membranous nephropathy. J Am Soc Nephrol. 2005;16:1195-1204.

15. You YH, Quach T, Saito R, et al. Metabolomics reveals a key role for fumarate in mediating the effects of NADPH oxidase 4 in diabetic kidney disease. J Am Soc Nephrol. 2016;27:466-481.

16. Isaacs JS, Jung YJ, Mole DR, et al, HIF overexpression correlates with biallelic loss of fumarate hydratase in renal cancerl novel role of fumarate in regulation of HIF stability. Cancer Cell. 2005;8:143-153.

17. Shanmugasndaram K, Nayak B, Shim EH, et al. The oncometabolite fumarate promotes pseudohypoxia through noncanonical activation of NF-kB signaling. J Bio Chem. 2014;289:24691-24699.

18. Kim Y, Han B-G, KoGES group. Cohort profile: The Korean genome and Epidemiology Study (KoGES) Consortium. Int J Epidemiol. 2017;46:e20.

19. De Vriese AS, Glassock RJ, Nath KA, et al. A proposal for a serology-based approach to membranous nephropathy. J Am Soc

Nephrol. 2016;28:421-430.


20. Tomas NM, Hoxha E, Reinicke AT, et al. Autoantibodies against thrombospondin type 1 domain-containing 7A induce membranous nephropathy. J Clin Invest. 2016;126:2519-2532.


21. Yang SH, Choi JW, Huh D, et al. Roles of fluid shear stress and retinoic acid in the differentiation of primary cultured human podocytes. Exp Cell Res. 2017;361:11-21.


22. Chen ZH, Qin WS, Zeng CH, et al. Triptolide reduces proteinuria in experimental membranous nephropathy and protects against C5b-9 induced podocyte injury in vitro. Kidney Int. 2010;77:974-988.


23. Qin H-Z, Zhang M-C, Le W-B, et al. Combined assessment of phospholipase A2 receptor autoantibodies and glomerular deposits in membranous nephropathy. J Am Soc Nephrol. 2016;27:3195-3203.


24. Zhou L, Chen X, Lu M, et al. Wnt/β-catenin links oxidative stress to podocyte injury and proteinuria. Kidney Int. 2019;95:830-845.


25. Li Y, Kang YS, Dia C, et al. Epithelial-to-mesenchymal transition is a potential pathway leading to podocyte dysfunction and

proteinuria. Am J Pathol. 2008;172:299-308.


26. Ashrafian H, Czibik G, Bellahcene M, et al. Fumarate is cardioprotective via activation of the Nrf2 antioxidant pathway. Cell Metab. 2012;15:361-371


27. Pollard P, Briere J, Alam N, et al. Accumulation of Krebs cycle intermediates and over-expression of HIFα in tumors which result from germline FH and SDH mutations. Hum Mol Genet. 2005;14:2231-2239.


28. Sullivan LB, Martinez-Garcia E, Nguyen H, et al. The proto-oncometabolite fumarate binds glutathione to amplify ROS-dependent signaling. Molecular cell. 2013;20:236-248.


29. Sciacovelli M, Goncalvs E, Johnson TI, et al. Fumarate is an epigenic modifier that elicits epithelial-to-mesenchymal transition. Nature. 2016;537:544-547.


30. Hu J-R, Coresh J, Inker LA, et al. Serum metabolites are associated with all-cause mortality in chronic kidney disease. Kidney Int. 2018;94:381-389.


31. Sedeek M, Nasrallah R, Touyz R.M, et al. NADPH oxidases, reactive oxygen spcies, and the kidney: friend and foe. J Am Soc

Nephrol. 2013;24:1512-1518.

32. Sendeyo K, Audard V, Zhang S-Y, et al. Upregulation of c-mip is closely related to podocyte dysfunction in membranous nephropathy. Kidney Int. 2013;83:414-425.

33. Reidy K, Susztak K. Epithelial-mesenchymal transition and podocyte loss in diabetic kidney disease. Am J Kidney Dis. 2009;54:590-593.

34. Asfahani RI, Tahoun MM, Miller-Hodges EV, at al. Activation of podocyte Notch mediates early Wt1 glomerulopathy. Kidney Int. 2018;93:903-920.

35. Guo Y, Pace J, Li Z, et al. Podocyte-specific induction of Krüppel-like factor 15 restores differentiation markers and attenuates kidney injury in proteinuric kidney disease. J Am Soc Nephrol. 2018;29:2529-2545.

36. Li J, Chen Y, Shen L, et al. Improvement of membranous nephropathy by inhibition of miR-193a to affect podocytosis via targeting WT1. J Cell Biochem. 2018;120:3348-3446.

37. Zheng L, Cardaci S, Jerby L, et al. Fumarate induces redox-dependent senescence by modifying glutathione metabolism. Nat

Commun. 2015;6:6001.

38. Hunt JL, Pollak MR, Denker BM. Cultured podocytes establish a size-selective barrier regulated by specific signaling pathways and demonstrate synchronized barrier assembly in a calcium switch model of junction formation. J Am Soc Nephrol. 2005;16:1593-1602.

39. Liu G, Kaw B, Kurfis J, et al. Neph1 and nephrin interaction in the slit diaphragm is an important determinant of glomerular permeability. J Clin Invest. 2003;112:209-221.

40. Murtas C, Bruschi M, Candiano G, et al. Coexistence of different circulating anti-podocyte antibodies in membranous nephropathy. Clin J Am Soc Nephrol. 2012;7:1394-1400.

41. Ternette N, Yang M, Laroyia M, et al. Inhibition of mitochondrial aconitase by succination in fumarate hydratase deficiency. Cell Rep. 2013;3:689-700.

42. Raimundo N, Baysal BE, Shadel GS. Revisiting the TCA cycle: signaling to tumor formation. Trends Mol Med. 2011;17:641-649.

# 국문 초록

막성신증에서 phospholipase A2 (PLA2) 수용체 자가면역에 따른 족세포 손상의 기전에 대해서는 밝혀져 있지 않다. 족세포 손상을 일으키는 기전 중 활성산소종이 작용할 것이라는 기존의 연구가 있으며 막성신증에서 활성산소종을 생성하는 보체계 활성화가 알려져 있다. 활성산소종과 관련된 물질 중 푸마르산은 최근 연구에서 족세포 손상에 관여하는 것으로 밝혀졌다. 본 연구에서는 PLA2 수용체 관련 막성신증 세포 모델에서 PLA2R 수용체 자가면역 유도에 따른 족세포 손상의 기전에 푸마르산이 관여한다는 가설을 세웠다.

푸마르산을 대사하는 효소인 푸마라아제 활성이 정상 신장조직의 사구체에서는 포도칼릭신과 병합되어 잘 나타났지만, PLA2 수용체 관련 막성신증 환자의 신장조직의 사구체에서는 정상 신장조직, PLA2 수용체 비관련 막성신증 환자, 미세변화신증 환자의 신장조직에서의 사구체 푸마라아제 활성과 비교하여 감소하는 것을 확인하였다.

생체 외 실험을 위해 막성신증 환자 중에서 혈청 항 PLA2 수용체 항체 역가가 양성인 환자와 정상인에게서 혈청을 얻어 각각의 혈청으로부터 면역 글로불린 G 를 정제하였다. 세포 실험을 위해서 신장절제술을 받은 환자에게서 얻은 신장조직에서 일차 배양한 사람의 족세포를 사용하였다. 각각의 면역 글로불린 G 와, 사람 족세포에서 추출한 단백질을 이용하여 웨스턴 블랏을 시행하였고 항 PLA2 수용체 항체 역가가 양성인 환자의 혈청에서 정제한 면역 글로불린 G 로 자극한 족세포에서만 항 PLA2 수용체 밴드를 153 kDa 위치에서 확인하였다.

항 PLA2 수용체 항체 역가가 양성인 환자의 혈청에서 정제한 면역 글로불린 G 로 자극한 족세포에서는 푸마라아제 활성이 감소한 것을

웨스턴 블랏으로 확인하였고 정상인 혈청에서 정제한 면역 글로불린 G 로 자극한 족세포와 비교하여 푸마르산 농도가 증가하였다. 이러한 변화는 족세포 형질전환에 관여하는 물질인 WT1, ZO-1 의 감소, Snail, 그리고 Fibronectin의 증가, 그리고 족세포 층을 가로지르는 알부민 유량의 증가, 활성산소종의 증가와 동반하였다.

이러한 족세포내의 WT1, ZO-1 의 단백질 발현의 감소는 푸마라아제 lentiviral particles를 처리하여 족세포의 푸마라아제 활성을 증가시켰을 때에는 회복되었으며 증가되었던 Snail 과 Fibronectin 단백질 발현과 활성산소종의 생성은 감소하였다. Small interfering RNA 를 사용하여 족세포에서 푸마라아제 활성을 감소시켰을 때에는 항 PLA2 수용체 항체 역가가 양성인 환자의 혈청에서 정제한 면역 글로불린 G 로 자극한 족세포에서 감소한 푸마라아제 활성이 더욱 감소하였고 더불어 WT1, ZO-1 의 약화된 발현이 더욱 약화되고, 증가한 fibronectin 과 Snail 의 단백질 발현 활성산소종의 생성이 더욱 증가하는 것을 확인하였다.

본 연구에서는 PLA2 수용체 매개 자가면역에 따라 족세포에서 감소되는 푸마라아제의 활성, 증가된 푸마르산의 결과로 족세포 표현형 변화가 유도되어 족세포 손상에 영향을 미치는 것을 확인하였다. 이러한 결과는 푸마르산이 PLA2 수용체 관련 막성신증 치료의 표적이 될 수 있는 것을 시사한다.

주요어 : 푸마르산, phospholipase A2 수용체 관련 막성신증, 족세포
학 번 : 2015-30559